JOURNAL OF GUIDANCE, CONTROL, AND DYNAMICS
Vol. 30, No. 2, March–April 2007

Relative Motion Between Satellites on Neighboring Keplerian Orbits

Philip L. Palmer* and Egemen İmre†
Surrey Space Centre, University of Surrey, Guildford, GU2 7XH England, United Kingdom

DOI: 10.2514/1.24804

In this paper, we explore the relative motion between two satellites on Keplerian orbits. We assume that the orbital elements defining the Keplerian ellipses for the two satellites are similar, so that we may neglect differences in these elements to second order. Analytic solutions for the relative motion are presented that conserve relevant quantities related to the Keplerian motions, and we discuss in detail the choice of initial conditions to improve the order of the approximations involved. Finally, we present results that compare our analytic results with differences of Keplerian orbits to determine the accuracy of the approximation, which is shown to be much greater than anticipated. An advantage of the approach presented over previous work in this area is that the relative motion is described in an inertial frame and not a rotating frame. This enables the effects of perturbations on the relative motion to be incorporated in a straightforward manner.

I. Introduction

THE analysis and modeling of the relative motion between two satellites is of immediate interest to allow the design and development of multiple satellite missions, such as satellite constellations and formations. Although the former is a more mature technology, close proximity precision formation flying has yet to be proven in space. Nevertheless, illustrating massive interest in this area, Xiang and Jørgensen [1] very recently published a survey of planned and existing formation flying missions, listing as many as 15 missions from the year 2000 to the year 2015 and beyond. The NASA EO-1 [2,3] remote sensing mission and the GRACE [4] mission mapping Earth's gravity field are two recent examples of the simple leader–follower type of large (several hundred kilometers) separation formations already in orbit.

On the other hand, there are proposed missions using interferometry, such as the Centre National dEtudes Spatiales (CNES) Interferometric Cartwheel [5] and the NASA and ESA joint-venture laser interferometer space antenna (LISA) technology demonstrator, LISA Pathfinder [6] (also known as SMART-2). In interferometry missions, the satellites are in a tightly controlled formation, with the very accurately maintained separation becoming the effective antenna size. It follows that, to meet the navigational accuracy demands of such missions, high-precision relative motion models are called for.

Perhaps the most well-known relative motion model is Hill's equations [7], adapted to the problem of relative satellite navigation by Clohessy and Wiltshire [8] in the 1960s, which essentially involved linearizing the Keplerian relative dynamics around a circular reference orbit. However, six years before Clohessy and Wiltshire, Lawden [9] (cf. [10]) derived the basic equations of relative motion for the more general case of eccentric orbits. Tschauner and Hempel [11] independently formulated similar solutions to Lawden's around the same time. The approach is, in fact, a generalization of the Clohessy–Wiltshire equations, solving the same problem, but linearizing around an eccentric orbit rather than a circular one. Although they still use Hill's frame, they employ true anomaly as the independent variable. Until recently, these solutions remained the only ones available to describe the relative motion in eccentric orbits.

There has been renewed interest in relative motion modeling within the last decade, because formation flying missions are becoming a reality. Broucke [10] solved the linearized relative motion equations using time as the independent variable, formulating the problem differently and deriving a time-explicit state transition matrix via partial derivatives of the reference orbit coordinates with respect to its orbital elements. Melton [12] attempted to provide time-explicit solutions for the relative motion. His method is similar to the Hill's equations approach but, rather than assuming a perfectly circular reference orbit, he includes e and e^2 expansion terms in the relative acceleration. He presents his end result in the form of a state transition matrix, albeit a rather complicated one.

Other researchers have included the effects of the linearized J_2 Earth oblateness term to the relative motion [13–16], as well as higher-order geopotential terms [17–20] and nonlinearity effects [21,22].

There are a few common threads that can be identified within the existing literature in the relative motion field. The first is that virtually all of the methods use a rotating and accelerating local coordinate frame. This approach makes analysis and visualization of the motion rather straightforward. However, the perturbations to the Keplerian potential are usually defined in the Earth-centered inertial (ECI) or, sometimes, in the rotating Earth-centered–Earth-fixed (ECEF) coordinate frames. This is one of the primary reasons why the addition of the simple J_2 perturbation term greatly complicates the equations. Therefore, the modeling of the motion is actually hampered by the employment of this accelerating rotating frame.

Perhaps more important, these methods do not explicitly address the issue of constants of the motion. For the motion of a satellite under a Keplerian potential, the energy and the angular momentum are both conserved. The same is true for the case of the two satellites: the relative energy and the relative angular momentum should also be conserved. If these quantities are not conserved, the relative orbits will get distorted over time. For example, any deviation from the relative energy will manifest itself as an along-track drift. In fact, a significant part of the relative positioning errors observed in the literature are down to the errors in relative energy, because the forces are integrated in a way that does conserve some constants, though they do not correspond to the real constants of the motion. Therefore, imposing these conservation laws should increase the accuracy and duration of the validity of the relative orbit propagator.

In this paper, we present a novel approach to modeling the relative motion of two satellites on neighboring elliptic orbits. We define a

Received 25 April 2006; revision received 19 September 2006; accepted for publication 21 September 2006.

*University Reader. Member AIAA.
†Currently Senior Researcher at TÜBİTAK-UZAY Space Technologies Research Institute, Ankara, Turkey; egemen.imre@uzay.tubitak.gov.tr.

relative angular momentum as well as a relative Hamiltonian and linearize these quantities. We then use the well-known Hamilton's equations to derive the equations of relative motion. Integrating analytically, the resulting expressions for relative position and velocity conserve the relative angular momentum as well as the relative energy. The derivation is carried out and the results are presented in the nonrotating perifocal frame to facilitate the incorporation of the perturbation terms within future work. Note that although the Keplerian force model may seem limiting, we have already extended this method to a high-precision numerical relative orbit propagator that can accommodate a complex geopotential model as well as other perturbations. This will be presented in a future publication.

The next section describes how the relative Hamiltonian and relative angular momentum are defined, as well as the derivation of the equations of motion and conservation of the constants of the motion. Section III describes how the equations of motion are integrated analytically to get relative position and velocity solutions. The following section details how the initial conditions can be chosen to improve the accuracy. Finally, we present the results of the proposed method.

II. Hamiltonian Description of Relative Motion

In this section, we shall consider the relative motion between two satellites moving in a Keplerian potential. Our approach is based on the Hamiltonian description of the motion, and our discussions focuses upon the conserved quantities of the motion. We start by considering a satellite at position $\boldsymbol{r}$ moving with velocity $\boldsymbol{v}$ in a Keplerian potential. The Hamiltonian for this satellite is given by

$$H = \frac{1}{2}(\boldsymbol{v}\cdot\boldsymbol{v}) - \frac{\mu}{r} \tag{1}$$

where μ is the gravitational parameter defining the potential, and r is the magnitude of the position vector $\boldsymbol{r}$. The position and velocity of this satellite define coordinates in a six-dimensional phase space, and Hamilton's equations define the motion of the satellite through this phase space at all later times. Now suppose that instead of a single satellite, there are two satellites in close proximity to each other in this phase space. We can define the position and velocity of these two satellites as $\boldsymbol{r} \pm \frac{1}{2}\delta\boldsymbol{r}$ and $\boldsymbol{v} \pm \frac{1}{2}\delta\boldsymbol{v}$. This description locates the midpoint in phase space as defined by $\boldsymbol{r}$ and $\boldsymbol{v}$ and the deviation from this midpoint for each of the two satellites. Consider the first-order Hamiltonian that describes the motion of the satellite for which the small increments in phase space coordinates are added to the midpoint coordinates:

$$H_1 = \frac{1}{2}(\boldsymbol{v}\cdot\boldsymbol{v}) + \frac{1}{2}(\boldsymbol{v}\cdot\delta\boldsymbol{v}) - \frac{\mu}{r}\left[1 - \frac{1}{2}\frac{\boldsymbol{r}\cdot\delta\boldsymbol{r}}{\boldsymbol{r}\cdot\boldsymbol{r}}\right] \tag{2}$$

The first-order Hamiltonian for the second satellite (H_2) can be found from the preceding by reversing the signs of $\delta\boldsymbol{r}$ and $\delta\boldsymbol{v}$. According to the theory of Hamiltonian systems, both of these quantities are conserved by the motion. We would, therefore, like to find a description of the relative motion that also conserves these quantities and exploits the fact that the separations in phase space are small. If we add these two Hamiltonians together, we obtain

$$H_1 + H_2 = 2\left(\frac{1}{2}\boldsymbol{v}\cdot\boldsymbol{v} - \frac{\mu}{r}\right) = 2H \tag{3}$$

where H is the Hamiltonian associated with the motion of the midpoint through phase space. The relative energy is defined as the difference between these two energies:

$$H_R = H_1 - H_2 = \boldsymbol{v}\cdot\delta\boldsymbol{v} + \frac{\mu}{r^3}(\boldsymbol{r}\cdot\delta\boldsymbol{r}) \tag{4}$$

The important point to note in this expression is that by our choice of describing the motion in terms of the phase space midpoint, the second-order terms in H_R would have cancelled even if they were computed in H_1 and H_2. Hence, the relative energy is accurate to third order.

We can think of the relative motion of the two satellites as a motion in a 12-dimensional phase space defined by the position and velocity of the midpoint and the separation positions and velocities. In this context, we may generalize the set of Hamilton's equations to obtain the following set in 12 dimensions:

$$\dot{\boldsymbol{r}} = \frac{\partial H_R}{\partial \delta\boldsymbol{v}} \qquad \dot{\boldsymbol{v}} = -\frac{\partial H_R}{\partial \delta\boldsymbol{r}} \tag{5}$$

$$\delta\dot{\boldsymbol{r}} = \frac{\partial H_R}{\partial \boldsymbol{v}} \qquad \delta\dot{\boldsymbol{v}} = -\frac{\partial H_R}{\partial \boldsymbol{r}} \tag{6}$$

These equations resemble the Hamilton's equations in six dimensions, but there is a cross-coupling between the relative motion and absolute motion of the midpoint.

Consider the equations of motion of the midpoint, which reduce to

$$\ddot{\boldsymbol{r}} + \frac{\mu}{r^3}\boldsymbol{r} = 0 \tag{7}$$

which is just Keplerian motion. The solution of this equation can be described in terms of two constant vectors: the angular momentum vector $\boldsymbol{L}$ and the eccentricity vector $\boldsymbol{e}$. The solution satisfies the equation of an ellipse:

$$r + \boldsymbol{e}\cdot\boldsymbol{r} = p \tag{8}$$

where p is the parameter that is dependent upon the magnitude of $\boldsymbol{L}$.

If we now consider the relative motion associated with these equations, then we can easily show that H_R is a conserved quantity:

$$\frac{\mathrm{d}H_R}{\mathrm{d}t} = \frac{\partial H_R}{\partial \boldsymbol{r}}\cdot\dot{\boldsymbol{r}} + \frac{\partial H_R}{\partial \boldsymbol{v}}\cdot\dot{\boldsymbol{v}} + \frac{\partial H_R}{\partial \delta\boldsymbol{r}}\cdot\delta\dot{\boldsymbol{r}} + \frac{\partial H_R}{\partial \delta\boldsymbol{v}}\cdot\delta\dot{\boldsymbol{v}} = 0 \tag{9}$$

A second quantity that is conserved in a Keplerian orbit is the orbital angular momentum $\boldsymbol{L}$. Consider the angular momentum associated with the first satellite:

$$\boldsymbol{L}_1 = (\boldsymbol{r} + \tfrac{1}{2}\delta\boldsymbol{r}) \times (\boldsymbol{v} + \tfrac{1}{2}\delta\boldsymbol{v}) \tag{10}$$

Expanding this to first order gives

$$\boldsymbol{L}_1 = \boldsymbol{L} + \tfrac{1}{2}(\boldsymbol{r}\times\delta\boldsymbol{v}) - \tfrac{1}{2}(\boldsymbol{v}\times\delta\boldsymbol{r}) \tag{11}$$

Again, the angular momentum of the second satellite is found by reversing the sign of the terms in the phase space separation. As with the energy, we can consider the sum of these terms as

$$\boldsymbol{L}_1 + \boldsymbol{L}_2 = 2\boldsymbol{L} \tag{12}$$

which is just the angular momentum of the Keplerian motion associated with the midpoint location. The relative angular momentum is then

$$\boldsymbol{L}_R = \boldsymbol{L}_1 - \boldsymbol{L}_2 = \boldsymbol{r}\times\delta\boldsymbol{v} - \boldsymbol{v}\times\delta\boldsymbol{r} \tag{13}$$

We can show that this quantity is also conserved by our equations of motion. Taking the time derivative and using Eq. (4), we have

$$\frac{d}{\mathrm{d}t}(\boldsymbol{r}\times\delta\boldsymbol{v}) = \boldsymbol{v}\times\delta\boldsymbol{v} - \frac{\mu}{r^3}(\boldsymbol{r}\times\delta\boldsymbol{r}) \tag{14}$$

Similarly,

$$\frac{d}{\mathrm{d}t}(\boldsymbol{v}\times\delta\boldsymbol{r}) = -\frac{\mu}{r^3}(\boldsymbol{r}\times\delta\boldsymbol{r}) + \boldsymbol{v}\times\delta\boldsymbol{v} \tag{15}$$

Hence, substituting into Eq. (13) shows that L_R is also a conserved quantity.

III. Description of the Relative Motion

In the preceding section, we derived a set of differential equations that describe the motion of a pair of satellites in terms of the motion of the midpoint and the evolution of the separation. The motion of the midpoint satisfies the equations for Keplerian motion and, hence, can be described analytically. The equations for the separation now need to be solved for. We have, however, demonstrated that these solutions conserve a relative energy and a relative angular momentum. These conservation laws are to be expected following conservation of energy and angular momentum of the individual satellite orbits.

We shall consider the solution of the relative equations, and first we need to decide which coordinate frame to use. Because the midpoint moves on a Keplerian orbit, it makes sense to use one coordinate axis (z axis) along the angular momentum vector $\boldsymbol{L}$ of this orbit. Another direction (x axis) points along the eccentricity vector $\boldsymbol{e}$ of this orbit. The third axis is then chosen to complete the right-handed set. The equations of relative motion are

$$\delta\dot{\boldsymbol{r}} = \delta\boldsymbol{v} \qquad \delta\dot{\boldsymbol{v}} = -\frac{\mu}{r^3}\delta\boldsymbol{r} + \frac{3\mu}{r^5}(\boldsymbol{r}\cdot\delta\boldsymbol{r})\boldsymbol{r} \tag{16}$$

If we now take the dot product of these equations with the unit vector along the z axis, then because $\boldsymbol{r}$ lies on the plane $z = 0$, we have

$$\delta\ddot{z} + \frac{\mu}{r^3}\delta z = 0 \tag{17}$$

where $\delta z = \delta\boldsymbol{r}\cdot\boldsymbol{k}$. If the angle between $\boldsymbol{r}$ and $\boldsymbol{e}$ is θ, then we can replace time as the independent variable by θ. This equation becomes

$$(1 + e\cos\theta)\frac{^2\mathrm{d}\delta z}{\mathrm{d}\theta^2} - 2e\sin\theta\frac{\mathrm{d}\delta z}{\mathrm{d}\theta} + \delta z = 0 \tag{18}$$

By changing variable to $R(\theta)$ such that $R = \delta z/r$, this equation simplifies to

$$\frac{d^2R}{\mathrm{d}\theta^2} + R = 0 \tag{19}$$

which provides the solution

$$\frac{\delta z}{r} = C\cos\theta + D\sin\theta \tag{20}$$

where parameters C and D are simply integration constants. Hence, the motion of the satellites around the orbit plane of the midpoint is a simple oscillation, which is the same solution as that obtained from Hill's equations for the limit of zero eccentricity.

Now consider the other components of $\delta\mathbf{r}$. We note that in the coordinates we are using, both $\boldsymbol{r}$ and $\boldsymbol{v}$ have no z component. We can then expand Eq. (4) as

$$H_R = \dot{x}\delta\dot{x} + \dot{y}\delta\dot{y} + (\mu/r^3)(x\delta x + y\delta y) \tag{21}$$

Similarly, the expression for the relative angular momentum can be written as

$$L_R = (x\delta\dot{y} - \delta y\dot{x}) + (\delta x\dot{y} - y\delta\dot{x}) \tag{22}$$

Because both of these quantities are conserved, we have the first integrals of the relative motion equations and only need to solve these coupled first-order equations for δx and δy. Once again, we express the components of the midpoint position and velocity in terms of its true anomaly θ and use this as the independent variable. These equations then reduce to the following forms:

$$\begin{aligned} &-\sin\theta\frac{\mathrm{d}\delta x}{\mathrm{d}\theta} + (e + \cos\theta)\frac{\mathrm{d}\delta y}{\mathrm{d}\theta} + (\delta x\cos\theta + \delta y\sin\theta) \\ &\quad = \frac{p^3H_R}{L^2}\frac{1}{(1 + e\cos\theta)^2} \end{aligned} \tag{23}$$

and

$$\begin{aligned} &-(1 + e\cos\theta)\sin\theta\frac{\mathrm{d}\delta x}{\mathrm{d}\theta} + (1 + e\cos\theta)\cos\theta\frac{\mathrm{d}\delta y}{\mathrm{d}\theta} \\ &\quad + (e + \cos\theta)\delta x + \sin\theta\delta y = \frac{pL_R}{L} \end{aligned} \tag{24}$$

We need to disentangle these equations to remove δx and its derivative. It is convenient to introduce $w = \cos\theta$ as an independent variable and to introduce new unknowns: $P = \delta x/r$ and $Q = \delta y/r$. These equations can then be rewritten in the following forms:

$$\frac{L_R}{L} = \left[(1 - w^2)\frac{\mathrm{d}P}{\mathrm{d}w} + wP\right] - \sqrt{1 - w^2}\left[w\frac{\mathrm{d}Q}{\mathrm{d}w} - Q\right] \tag{25}$$

and

$$\begin{aligned} \frac{p^2H_R}{L^2} &= (1 + ew)\left[(1 - w^2)\frac{\mathrm{d}P}{\mathrm{d}w} + wP\right] \\ &\quad - e(1 - w^2)P - e\sqrt{1 - w^2}\left[\frac{\mathrm{d}Q}{\mathrm{d}w} - wQ\right] \\ &\quad - \sqrt{1 - w^2}(1 + ew + e^2)\left[w\frac{\mathrm{d}Q}{\mathrm{d}w} - Q\right] \end{aligned} \tag{26}$$

We can now substitute the first bracket in Eq. (25) into Eq. (26) and solve for P:

$$\begin{aligned} (1 - w^2)P &= \frac{1}{eL}\left[(1 + ew)L_R - \frac{p^2H_R}{L}\right] \\ &\quad - \sqrt{1 - w^2}\left[(1 + ew)\frac{\mathrm{d}Q}{\mathrm{d}w} - (e + w)Q\right] \end{aligned} \tag{27}$$

We can also rewrite Eq. (25) in the following form:

$$(1 - w^2)^{3/2}\frac{d}{\mathrm{d}w}\left[\frac{P}{\sqrt{1 - w^2}}\right] = \frac{L_R}{L} + \sqrt{1 - w^2}\left[w\frac{\mathrm{d}Q}{\mathrm{d}w} - Q\right] \tag{28}$$

To complete the elimination, we divide Eq. (27) by $(1 - w^2)^{3/2}$ and differentiate. Substituting the result into Eq. (28) then leaves us with a differential equation for $Q(\theta)$:

$$(1 - w^2)\frac{d^2Q}{\mathrm{d}w^2} + 2w\frac{\mathrm{d}Q}{\mathrm{d}w} - 2Q = \frac{3w}{\sqrt{1 - w^2}}\left[\frac{L_R}{eL} - \frac{p^2H_R}{eL^2}\frac{1}{1 + ew}\right] \tag{29}$$

The solution of this differential equation is straightforward, if lengthy, but the general solution is

$$\begin{aligned} Q &= A(1 + w^2) + Bw - \frac{L_R}{eL}w\sqrt{1 - w^2} \\ &\quad + \frac{p^2H_R}{eL^2}\frac{1}{1 - e^2}\left[\frac{e(2 + e^2) + w(1 + 2e^2)}{1 - e^2}\sqrt{1 - w^2}\right. \\ &\quad \left. - \frac{3eE}{(1 - e^2)^{3/2}}(e + w)(1 + ew)\right] \end{aligned} \tag{30}$$

where E is the eccentric anomaly of the midpoint orbit, and A and B are integration constants that can be found from the initial conditions. Some comment needs to be made on how the eccentric anomaly enters this equation; it appears through the evaluation of the following integral:

$$\int\frac{\mathrm{d}w}{\sqrt{1 - w^2}(1 + ew)} = \frac{\pi - E}{\sqrt{1 - e^2}} \tag{31}$$

Having found the solution for Q, we can substitute this result into Eq. (27) to find P. The result needs to be manipulated to remove apparent singularities that cancel when terms are grouped appropriately, leaving the result

$$P = \sqrt{1-w^2}[(e-w)A - B] + \frac{L_R}{eL}[2 + w(e-w)] + \frac{p^2 H_R}{eL^2}\frac{1}{1-e^2}\left[(1+ew+w^2) - \frac{3(1-e^2w^2)}{1-e^2} + \frac{3eE}{(1-e^2)^{3/2}}\sqrt{1-w^2}(1+ew)\right] \tag{32}$$

The emergence of the eccentric anomaly in these solutions requires us to solve Kepler's problem to find the relative positions at a given time. We note, however, that the components of velocity of the midpoint have the following form:

$$v_x = -\frac{L}{p}\sin\theta \tag{33}$$

and

$$v_y = \frac{L}{p}(e + \cos\theta) \tag{34}$$

This shows that the factors multiplying the eccentric anomaly in Eqs. (30) and (31) are the components of the midpoint velocity. If we further use the Kepler relation

$$\sin\theta = \frac{p}{r}\frac{\sin E}{(1-e^2)^{1/2}} \tag{35}$$

we can replace the eccentric anomaly in the preceding with the mean anomaly M. Our results then simplify to

$$\delta x = Ar\sin\theta(e - \cos\theta) - Br\sin\theta + \frac{L_R r}{eL}[2 + \cos\theta(e-\cos\theta)] + \frac{a^2 H_R}{eL^2}(1-e^2)\mathcal{P}$$
$$\delta y = Ar(1+\cos^2\theta) + Br\cos\theta - \frac{L_R r}{eL}\sin\theta\cos\theta + \frac{a^2 H_R}{eL^2}(1-e^2)\mathcal{Q} \tag{36}$$

where

$$\mathcal{P} = r\cos\theta(e + \cos\theta) - 2r - \frac{3a^2}{L}e\sqrt{1-e^2}v_x M \tag{37}$$

and

$$\mathcal{Q} = r\sin\theta(2e + \cos\theta) - \frac{3a^2}{L}e\sqrt{1-e^2}v_y M \tag{38}$$

We can rearrange these expressions in a more convenient form:

$$\mathcal{P} = 2ex - r[2 + \cos(e - \cos\theta)] - \frac{3a^2}{L}e\sqrt{1-e^2}v_x M \tag{39}$$

and

$$\mathcal{Q} = 2ey + r\sin\theta\cos\theta - \frac{3a^2}{L}e\sqrt{1-e^2}v_y M \tag{40}$$

We can then simplify our expressions for the relative position of the satellites to

$$\delta\boldsymbol{r} = \delta\boldsymbol{r}_p - \frac{H_R}{H}\left(\boldsymbol{r} - \frac{3}{2}\boldsymbol{v}t\right) \tag{41}$$

where $\delta\boldsymbol{r}_p = \delta x_p\boldsymbol{i} + \delta y\boldsymbol{j}$ is the periodic variation of the separation given by

$$\delta x_p = (eA - B)y - Ax\sin\theta + \frac{1}{eL}\left(L_R + \frac{H_R}{2H}L\right)(p + y\sin\theta)$$
$$\delta y_p = 2Ar + Bx - Ay\sin\theta - \frac{1}{eL}\left(L_R + \frac{H_R}{2H}L\right)x\sin\theta \tag{42}$$

This provides a very simple expression for the relative position of the satellites. To complete our analysis, we now consider the relative velocity between the satellites. Differentiating the preceding gives

$$\delta\boldsymbol{v} = \delta\boldsymbol{v}_p + \frac{H_R}{2H}\left(\boldsymbol{v} - \frac{3\mu}{r^3}\boldsymbol{r}t\right) \tag{43}$$

and the periodic part of the velocity reduces to

$$\delta\dot{x}_p = (eA - B)v_y - A\left(v_x\sin\theta + \frac{L}{r^2}x\cos\theta\right) + \frac{1}{eL}\left(L_R + \frac{H_R}{2H}L\right)\left(v_y\sin\theta + \frac{L}{r^2}y\cos\theta\right)$$
$$\delta\dot{y}_p = (B - 2eA)v_x - \frac{1}{eL}\left(L_R + \frac{H_R}{2H}L\right)\left(v_x\sin\theta + \frac{L}{r^2}x\cos\theta\right) - A\left(v_y\sin\theta + \frac{L}{r^2}y\cos\theta\right) \tag{44}$$

This completes the solution for the relative motion.

We note that these solutions have still a singularity as $e \to 0$, which corresponds to Hill's problem. We briefly show how these equations reduce to the usual Hill's equations in this limit. The reason the singularity arises in the solutions is because if the midpoint moves around a circular orbit, then H_R and L_R are related by

$$H_R = nL_R \tag{45}$$

where n is the angular rate of the motion of the midpoint. This means that in this case, we no longer have two independent differential equations. The preceding condition follows from the fact that for circular orbits, $HL^2 = -\mu^2/2$. Differentiating this result gives the relationship $\delta H = n\delta L$. The energy vs angular momentum plane has a forbidden region in which no orbits are possible. The bounding curve of this region is the set of circular orbits, and because the energy and angular momenta of our two satellites must be symmetrically placed about that of the midpoint, they must lie along the tangent to this curve. This is described by the preceding relation.

So when the midpoint moves along a circular orbit, we cannot use the angular momentum as independent information. From Eq. (20), we see that the z motion satisfies the solution of Hill's problem when r is constant. The in-plane motion can be found from Eqs. (5) that, in component form, reduce to

$$\delta\ddot{x} = -n^2\delta x - 3n^2\cos\theta(\delta x\cos\theta + \delta y\sin\theta) \tag{46}$$

$$\delta\ddot{y} = -n^2\delta y - 3n^2\sin\theta(\delta x\cos\theta + \delta y\sin\theta) \tag{47}$$

If we use rotated coordinates

$$u = \delta x\cos\theta + \delta y\sin\theta \qquad v = -\delta x\sin\theta + \delta y\cos\theta \tag{48}$$

then these equations can be written as the usual Hill equations

$$\ddot{u} - 2n\dot{v} + 3n^2 u = 0 \tag{49}$$

$$\ddot{v} + 2n\dot{u} = 0 \tag{50}$$

which proves that the analytic solutions developed here reduce to the more familiar Hill solutions for the circular case.

Table 1 Formation initial conditions in Keplerian elements

	a, km	e	I, deg	Ω, deg	ω, deg	θ, deg	H	L
Sat1	15945.800	≤ 0.3500	60.00	40.03	20.00	73.00	-0.199994	1.481152
Sat2	15945.650	≤ 0.3501	60.03	40.03	19.95	73.05	-0.199996	1.481086
Diff	-0.150	0.0001	0.030	0.030	-0.050	0.050	-1.881×10^{-6}	-6.605×10^{-5}

IV. Modeling Accuracy

A. Initial Conditions

In the preceding sections, we derived a solution for the relative motion between two satellites following arbitrary elliptic orbits. We now consider the 12 initial conditions: the position and velocity of the reference and the relative position and velocity. For the relative motion, we replace these initial conditions by the constant quantities A, B, C, D, H_R, and L_R. We note, however, that if $\theta = 0$ or π, then y vanishes, and from Eq. (42), δx_p becomes independent of both A and B. This is along the line of nodes of the reference orbit. Along this line, $v_x = 0$ also; hence, from Eq. (44), $\delta \dot{y}_p$ also becomes independent of A and B. It is, therefore, more useful to determine A and B from y_p and $\delta \dot{x}_p$. The constants C and D describing the cross-track motion are easily determined from

$$C = \delta z_0 p(e + \cos\theta_0) - \delta \dot{z}_0 \frac{p^3}{L} \frac{\sin\theta_0}{1 + e\cos\theta_0} \tag{51}$$

$$D = \delta z_0 p \sin\theta_0 + \delta \dot{z}_0 \frac{p^3}{L} \frac{\cos\theta_0}{1 + e\cos\theta_0} \tag{52}$$

The choice of the reference allows for some flexibility. Our analysis suggests that we should average the two satellite positions and velocities. This will induce a second-order error in the energy H and a third-order error in the relative energy H_R. Equation (41), however, has a secularly growing term that is dependent upon the difference in orbital energy. To maintain the accuracy of our linear approximations, we must minimize any errors in this secular term. This suggests that we should fix H_R to be exactly equal to $H_1 - H_2$. Also, the fact that $1/H \propto a$ appears in this expression suggests that we may find it better to set the semimajor axis of the reference orbit as the average of the values of a for the two satellite orbits.

What difference does this choice of setting the midpoint orbit have on our analysis? If we compute the average of the energies, then the semimajor axis of the midpoint orbit is given by $\langle a \rangle$, where

$$\frac{1}{\langle a \rangle} = \frac{1}{2}\left(\frac{1}{a_1} + \frac{1}{a_2}\right) \tag{53}$$

If $\bar{a} = (a_1 + a_2)/2$, then one can easily show that

$$\langle a \rangle = \bar{a} - \tfrac{1}{4}(a_1 - a_2)^2 \tag{54}$$

Hence, the difference in the choice is second order, and to the order of accuracy of our analysis, both should be valid. This inclusion of second order in the initial conditions changes how long our analytic solution is valid and how large our formation can be.

We have considered a number of alternative ways to choose the reference orbit and compared the accuracy of our analytic approximation to the difference of the two Keplerian orbits. Four cases have been considered: 1) averaging satellite positions and velocities, 2) averaging orbital energies and angular momentum vectors, 3) averaging the orbital elements of each satellite, and 4) averaging the eccentricity and angular momentum vectors. A simple formation scenario was used to compare these initialization methods. Table 1 details the initial conditions used. We considered the accuracy of the predicted relative position after five days, corresponding to 21 orbital periods. The difference in eccentricity of the two satellites was fixed at 0.001, although their eccentricities were allowed to vary. The formation starts with an initial separation of 8 to 9 km, depending upon the eccentricity. The 150-m semimajor axis difference causes the satellites to drift apart, reaching about 40-km separation by the end.

In Fig. 1, we see the relative position error as a function of the eccentricity of the orbits. We see that all the methods perform well. Averaging the position and velocity vectors (shown as posvel in the figure) yield accuracies around a few meters. Continuation of the propagation beyond five days, however, shows that this error grows quadratically with time. The same quadratic growth in error is also seen in averaging the eccentricity and angular momentum vectors (shown as e_h in the figure). The other two methods, namely, averaging the energies and angular momentum vectors (shown as en_h in the figure) and averaging the orbital elements (shown as elems in the figure), clearly outperform these, reducing the error to between 1–10% of the first two methods. The best method is averaging the orbital element sets, for which an accuracy around 10 cm is achieved after five days.

B. Correcting the Relative Hamiltonian and Angular Momentum

The second-order changes to the reference will change the quantity in Eq. (4) that is conserved by the equations of motion. This value will differ from $H_1 - H_2$, which is the correct conserved quantity. The error will become second order because of the second-order changes made to $\boldsymbol{r}$ and $\boldsymbol{v}$. This can be seen in Fig. 2, along with the resulting error in relative position after five days. The initial conditions for this experiment are given in Table 2, in which the two satellites started at true anomalies of 301 and 302 deg, respectively. We see from this figure that the relative position errors are directly

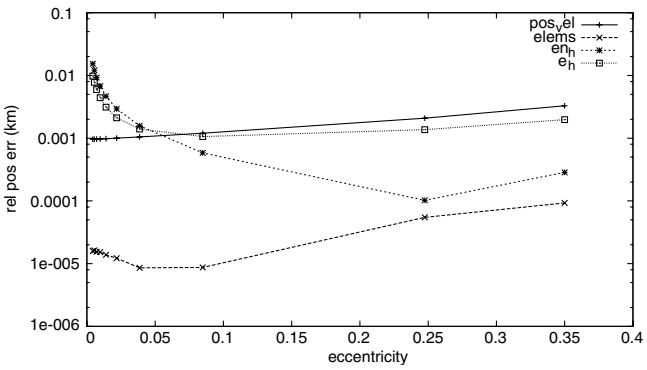

Fig. 1 Peak relative positioning error magnitude (in log scale) variation with eccentricity (21.5 orbits).

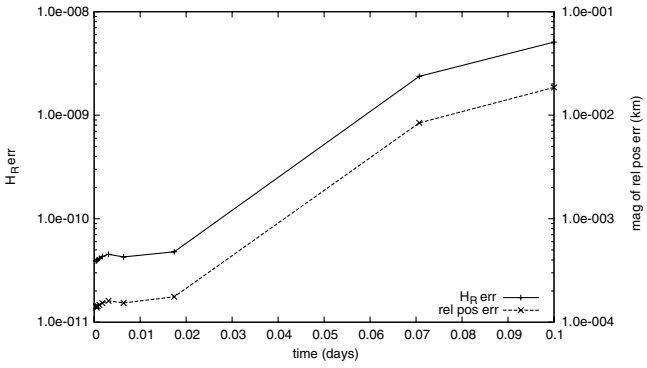

Fig. 2 Peak relative positioning error magnitude and H_R error variation (in log scale) with eccentricity (65 orbits).

Table 2 Formation initial conditions in Keplerian elements

	a, km	e	I, deg	Ω, deg	ω, deg	θ, deg	H	L
Sat1	7653.780	≤ 0.0050	60.00	40.0	20.0	61.0	-0.416665	1.095432
Sat2	7653.700	≤ 0.0055	60.01	40.0	19.0	62.0	-0.416670	1.095423
Diff	-0.080	0.0005	0.010	0.0	-1.0	1.0	-4.355×10^{-6}	-8.601×10^{-6}

proportional to the error in H_R. What is not seen in this figure is that this relative position error grows linearly with time. This means that we can predict from the outset what the positional errors will be at any future time, just based upon how accurately H_R matches the difference in orbital energies of the two satellites.

As shown in this example, 15-cm relative positioning accuracy is possible for a five-day propagation. To put the errors in perspective, it should be emphasized that the initial separations vary from about 10 km for higher eccentricities to about 1 km for lower eccentricities, and peak separations are about 65 km for high eccentricities and 50 km for low eccentricities.

To ensure a better match for H_R we need to reconsider Eq. (4). Because the relative position and velocity of the two satellites are fixed, we need to adjust the position and velocity of the reference point. The orbital parameters for the reference, however, were fixed in the preceding section. We have freedom, however, to adjust the true anomaly of the reference point along that orbit, and we can adjust the argument of perigee ω of the orbit.

First consider H_R and L_R, expressed in terms of the true anomaly along the reference orbit:

$$H_R = \frac{L}{p}[-\sin\theta\delta\dot{x} + (e + \cos\theta)\delta\dot{y}] + \frac{L^2(1 + e\cos\theta)^2}{p^4}[\cos\theta\delta x + \sin\theta\delta y] \tag{55}$$

$$L_R = \frac{-p}{(1 + e\cos\theta)}[\sin\theta\delta\dot{x} - \cos\theta\delta\dot{y}] + \frac{L}{p}[(e + \cos\theta)\delta x + \sin\theta\delta y] \tag{56}$$

By adjusting the starting value of θ, we can bring these quantities closer to the correct values.

For the argument of perigee, consider an inertial coordinate system, such as the well-known Earth-centered inertial frame. If we rewrite our perifocal coordinates in terms of this inertial frame, the argument of perigee ω will appear explicitly in the equations and therefore can be adjusted. For this, the δx and δy terms in Eqs. (55) and (56) can be replaced by their inertial counterparts δx_I and δy_I, such that

$$\delta x = \delta x_I \cos\omega + \delta y_I \sin\omega \tag{57}$$

$$\delta y = -\delta x_I \sin\omega + \delta y_I \cos\omega \tag{58}$$

The effect of these adjustments is shown in Fig. 3. Obviously, for smaller eccentricities, the effect of ω becomes very small and is unable to match both H_R and L_R. In this case, we restrict ourselves to correcting H_R only. If we fix the value of H_R to the correct value, then we need to solve a nonlinear equation for θ and ω, but in practice, a linearized approximation will suffice, because the adjustments in these angles will be small.

We tested the effectiveness of this correction term using the initial conditions given in Table 2. Figure 4 illustrates H_R and relative positional errors for both corrected (shown as corr) and uncorrected cases. As expected, H_R errors grow parallel to the relative positioning errors. H_R error is significantly lower in the corrected case and this results in relative positioning errors to be cut by about a factor of 3, increasing to a factor of 20 to 40 for larger eccentricities. Therefore, errors on the order of 30 to 60 m are cut to about 0.7 to 2.5 m, for a five-day propagation. This illustrates the effectiveness of correcting the phase of the reference orbit.

Similarly, Fig. 5 demonstrates the variation of the L_R error, for which the relative angular momentum varies between -5.7×10^{-6} for the smallest eccentricity to -1.7×10^{-5} for the largest. As can be seen, the corrected L_R yields vastly superior performance, practically matching the relative angular momentum.

Figure 6 illustrates the angular correction required to modify the H_R and L_R values for this case, in which true anomaly correction is shown as θ corr and the argument of perigee correction is shown as ω corr. For larger eccentricities, small angular corrections are adequate, because it is easier to manipulate the along-track and radial coordinates of the reference satellite with a small change. However, as the orbit becomes more circular, it takes progressively larger angular changes to alter H_R and L_R sufficiently. Such a large angular change in true anomaly was countered by a similar and opposite direction change in argument of perigee, in agreement with the discussion regarding Fig. 3.

We also considered the case when the difference in semimajor axis was larger, as per Table 1. Here, we used true anomalies of the satellites as 73 and 73.05 deg, respectively. Initial separations vary between 1.7 km at large eccentricities to about 9.6 km at small eccentricities. Because of the 150-m semimajor axis difference, separations increase rapidly in time, with peak separations between 35 to 70 km. Figure 7 presents a comparison of the H_R error with and without the correction terms applied (shown in the figure as H_R err corr and H_R err, respectively). When compared with the energy

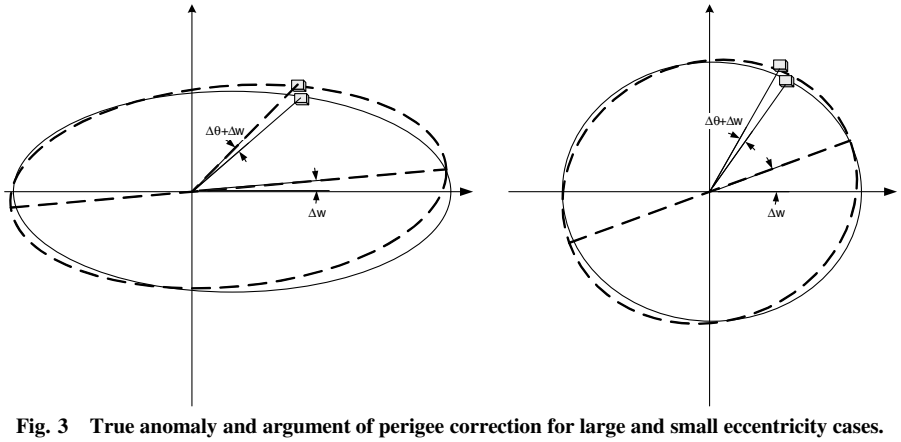

Fig. 3 True anomaly and argument of perigee correction for large and small eccentricity cases.

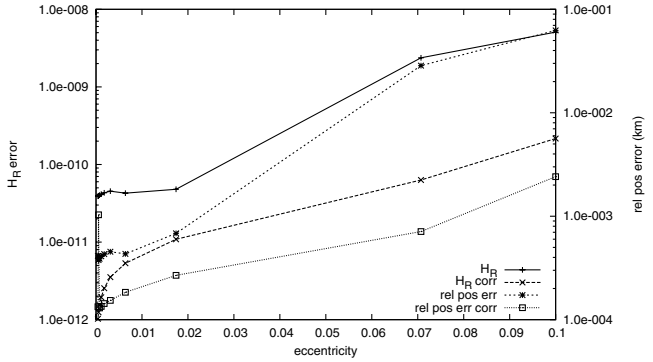

Fig. 4 H_R error variation and peak relative positioning error magnitude with/without corrections (in log scale) with eccentricity.

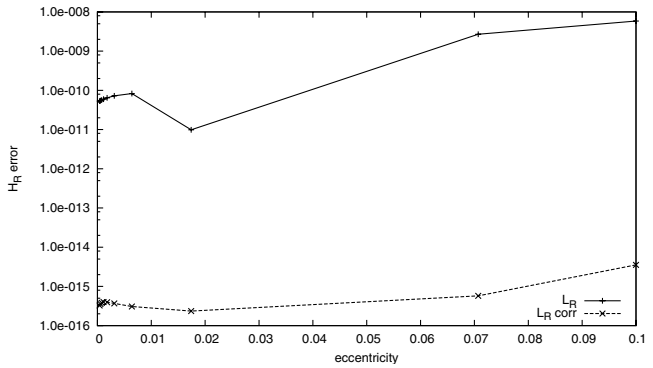

Fig. 5 L_R error variation with/without corrections (in log scale) with eccentricity.

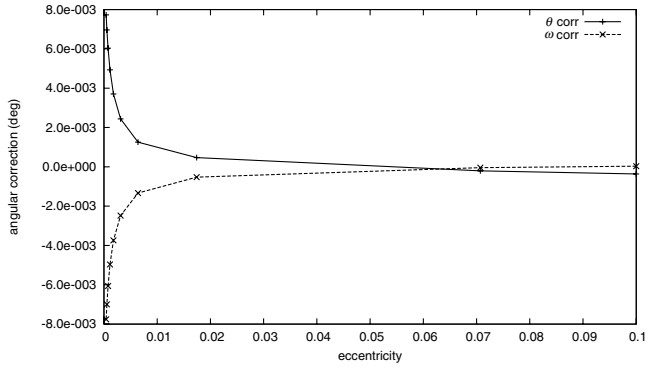

Fig. 6 True anomaly and argument of perigee correction with eccentricity (21.5 orbits).

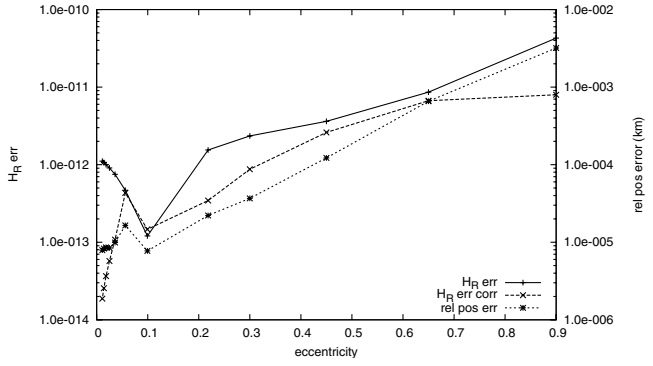

Fig. 7 H_R error variation with/without corrections and peak relative positioning error magnitude (in log scale) with eccentricity.

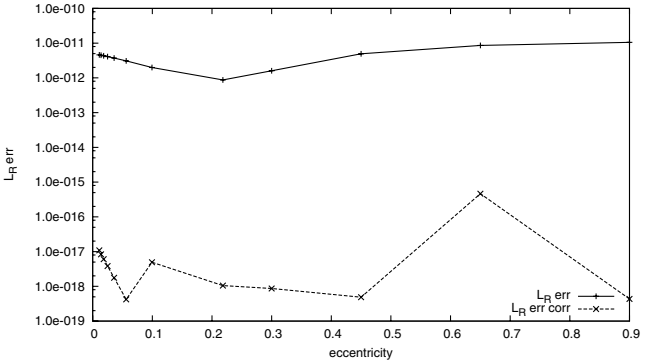

Fig. 8 L_R error variation with/without corrections (in log scale) with eccentricity.

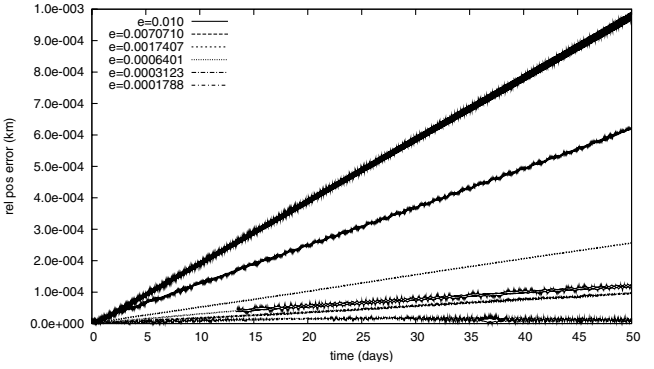

Fig. 9 Error in relative positioning for close proximity case (650 orbits).

difference of -1.8×10^{-6}, both corrected and uncorrected H_R values are very accurate. However, the correction term is seen to reduce the H_R error even further across the eccentricity spectrum. The figure also shows the relative positioning error when the correction terms are applied. As expected, the relative positioning error profile follows the H_R error and it exceeds the 1-m mark only for the $e = 0.9$ case.

Figure 8 shows the variation of the error in the L_R term. The relative angular momentum starts at about -9×10^{-6} for the 10^{-2} level eccentricities, increasing to -3×10^{-4} for the $e = 0.9$ case. Although the error in the uncorrected L_R (shown as L_R err in the figure) is already small compared with the real relative angular momentum, the corrected L_R is seen to practically match it.

C. Long-Term Stability

For most formation flying scenarios, the satellites will remain within a few kilometers of each other over long times. To evaluate the approximations we have used for such close proximity scenarios, we

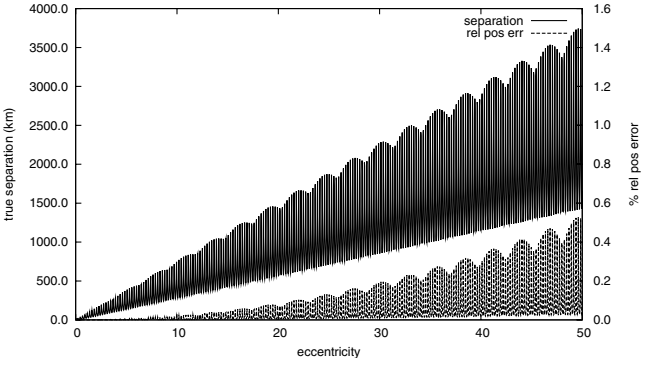

Fig. 10 True separation and percentage error in relative positioning (217 orbits).

used the initial conditions in Table 2, but without any difference in semimajor axis, to ensure that the satellites do not drift away. We again considered a range of eccentricities and evaluated the relative position after 50 days (650 orbits). The satellites stay within less than 3.5 km of each other. Figure 9 demonstrates the relative positioning error variation with time. Although the errors grow with increasing eccentricity, it takes 50 days for the largest error to exceed 1 m. For eccentricities around 0.001, the error is around 10 cm. This demonstrates the high accuracy of our approximation after correction of the initial conditions is made.

Encouraged by the achievements of this approximation over several days, we considered testing it over very long timescales when the satellites had drifted apart substantially. Once again, we set up initial conditions as in Table 1, with an eccentricity of 0.45 and an eccentricity difference of 0.001. We increased the semimajor axis difference to 1150 m, such that the separation between the satellites reached thousands of kilometers in 50 days (217 orbits). Figure 10 shows the separation between the satellites, which exceeds 3500 km. Even though the relative position error no longer grows linearly, it only reaches 0.5% of the total separation, corresponding to about 20 km. The initial H_R error is only -2.1×10^{-13}; however, the distance between the geometric midpoint of the satellite positions and the reference point reaches 140 km. Because we assume that the reference satellite stays near the geometric midpoint to the first order, the force acting on the satellites is evaluated at this location, then the increasing separation between these two points is likely the main source of error.

V. Conclusions

In this paper, we have presented an analytical solution for the relative motion of two satellites moving along similar Keplerian elliptic orbits, introducing a formal methodology based upon the conservation of relative Hamiltonian and relative angular momentum. The solutions to these dynamical equations are very simple expressions and separate the secular drift between the satellites from periodic oscillations in relative position around the reference orbit. This Keplerian model forms the starting point of a numerical relative orbit propagator that can accommodate a complex geopotential model as well as other perturbations. This propagator will be explained in detail in a future publication.

We have analyzed the choice of reference orbit about which our linearization is made and shown that by appropriately choosing second-order corrections in the initial conditions, the resulting analytic equations remain accurate to very high precision over periods of time lasting several months.

We have presented a detailed set of tests of the accuracy and robustness of our model for various challenging scenarios, with a wide range of eccentricities, proximities, and semimajor axes. We demonstrate accuracies between meter and centimeter level after several days, outperforming second-order models.

Acknowledgments

Egemen İmre has been supported by the Turkish research and development agency TÜBİTAK-UZAY and the Surrey Space Centre throughout this work.

References

[1] Xiang, W., and Jørgensen, J. L., "Formation Flying: A Subject Being Fast Unfolding in Space," 5th IAA Symposium on Small Satellites for Earth Observation, Berlin, Germany, International Academy of Astronautics Paper B5-0309P, 2005.

[2] Folta, D., Bristow, J., Hawkins, A., and Dell, G., "Enhanced Formation Flying Validation Report (GSFC Algorithm)," NASA Goddard Space Flight Center, 2002.

[3] Guinn, J., "Enhanced Formation Flying Validation Report (JPL Algorithm)," NASA Goddard Space Flight Center Rept. 02-0548, 2002.

[4] Tapley, B. D., Bettadpur, S., Watkins, M., and Reigber, C., "The Gravity Recovery and Climate Experiment: Mission Overview and Early Results," *Geophysical Research Letters*, Vol. 31, No. 9, 2004, pp. 1–4.

[5] Runge, H., Bamler, R., Mittermayer, J., Jochim, F., Massonnet, D., and Thouvenot, E., "The Interferometric Cartwheel for ENVISAT," 3rd IAA Symposium on Small Satellites for Earth Observation, Berlin, Germany, International Academy of Astronautics Paper B3-0607P, 2001.

[6] Landgraf, M., Hechler, M., and Kemble, S., "Mission Design for LISA Pathfinder," *Classical and Quantum Gravity*, Vol. 22, No. 10, 2005, pp. 487–492.

[7] Hill, G. W., "Researches in the Lunar Theory," *American Journal of Mathematics*, Vol. 1, No. 3, 1978, pp. 5–26, 129–147, 245–260.

[8] Clohessy, W., and Wiltshire, R., "Terminal Guidance System for Satellite Rendezvous," *Journal of the Aerospace Sciences*, Vol. 27, No. 9, 1960, pp. 653–658, 674.

[9] Lawden, D., "Fundamentals of Space Navigation," *Journal of the British Interplanetary Society*, Vol. 13, May 1954, pp. 87–101.

[10] Broucke, R., "Solution of the Elliptic Rendezvous Problem with the Time as Independent Variable," *Journal of Guidance, Control, and Dynamics*, Vol. 26, No. 4, 2003, pp. 615–621.

[11] Tschauner, J., and Hempel, P., "Optimale Beschleunigeungsprogramme fur das Rendezvous-Manover," *Acta Astronautica*, Vol. 10, Nos. 5–6, 1964, pp. 296–307.

[12] Melton, R., "Time-Explicit Representation of Relative Motion Between Elliptical Orbits," *Journal of Guidance, Control, and Dynamics*, Vol. 23, No. 4, 2000, pp. 604–610.

[13] Gim, D.-W., and Alfriend, K. T., "The State Transition Matrix for Relative Motion of Formation Flying Satellites," AAS Space Flight Mechanics Meeting, San Antonio, TX, American Astronautical Society Paper 02-186, 2002.

[14] Gim, D.-W., and Alfriend, K. T., "The State Transition Matrix of Relative Motion for the Perturbed Non-Circular Reference Orbit," *Guidance and Control*, Advances in the Astronautical Sciences, Vol. 108, American Astronautical Society, Springfield, VA, 2001, pp. 913–934; also American Astronautical Society Paper 01-222.

[15] Schaub, H., and Alfriend, K. T., "J_2 Invariant Relative Orbits for Spacecraft Formations," *Celestial Mechanics and Dynamical Astronomy*, Vol. 79, Feb. 2001, pp. 77–95.

[16] Schweighart, S., and Sedwick, R., "High-Fidelity Linearized J_2 Model for Satellite Formation Flight," *Journal of Guidance, Control, and Dynamics*, Vol. 25, No. 6, 2002, pp. 1073–1080.

[17] Kormos, T., "Dynamics and Control of Satellite Constellations and Formations in Low Earth Orbit," Ph.D. Thesis, Univ. of Surrey, Guildford, England, U.K., 2004.

[18] O'Donnell, K., "Satellite Orbits in Resonance with Tesseral Harmonics: Absolute and Relative Orbit Analysis," Ph.D. Thesis, Univ. of Surrey, Guildford, England, U.K., 2005.

[19] Kormos, T., and Palmer, P., "Modeling and Control of Relative Orbits for Spacecraft Flying in Formation in LEO," *Third International Workshop on Satellite Constellations and Formation Flying*, International Astronautical Federation, Paris, 2003, pp. 279–286.

[20] Wiesel, W., "Relative Satellite Motion About an Oblate Planet," *Journal of Guidance, Control, and Dynamics*, Vol. 25, No. 4, 2002, pp. 776–785.

[21] Karlgaard, C., and Lutze, F., "Second-Order Relative Motion Equations," *Journal of Guidance, Control, and Dynamics*, Vol. 26, No. 1, 2003, pp. 41–49.

[22] Vaddi, S., Vadali, S., and Alfriend, K., "Formation Flying: Accommodating Nonlinearity and Eccentricity Perturbations," *Journal of Guidance, Control, and Dynamics*, Vol. 26, No. 2, 2003, pp. 214–223.